Exploring the wavelength range of InP/AlGaInP QDs and application to dual-state lasing

Invited Article

Exploring the wavelength range of InP/AlGaInP QDs and application to dual-state lasing

Samuel Shutts[1], Stella N Elliott[1], Peter M Smowton[1] and Andrey B Krysa[2]

[1] School of Physics and Astronomy, Cardiff University, Cardiff, CF24 3AA, UK
[2] EPSRC National Centre for III-V Technologies, Department of Electronic and Electrical Engineering, University of Sheffield, Mappin Street, Sheffield, S1 3JD, UK

E-mail: shuttss@cardiff.ac.uk

CrossMark

Abstract

We explore the accessible wavelength range offered by InP/AlGaInP quantum dots (QD)s grown by metal–organic vapour phase epitaxy and explain how changes in growth temperature and wafer design can be used to influence the transition energy of the dot states and improve the performance of edge-emitting lasers. The self assembly growth method of these structures creates a multi-modal distribution of inhomogeneously broadened dot sizes, and via the effects of state-filling, allows access to a large range of lasing wavelengths. By characterising the optical properties of these dots, we have designed and demonstrated dual-wavelength lasers which operate at various difference-wavelengths between 8 and 63 nm. We show that the nature of QDs allows the difference-wavelength to be tuned by altering the operating temperature at a rate of up to $0.12 \, \text{nm} \, \text{K}^{-1}$ and we investigate the factors affecting intensity stability of the competing modes.

(Some figures may appear in colour only in the online journal)

1. Introduction

The most established quantum dot (QD) lasers are those formed from 1.3 to 1.6 μm emitting InAs/GaAs, where extensive research was stimulated by the technological demands of the telecommunication industry. More recently, InP-based QDs have emerged that cover a wavelength regime that extends from 650 nm to 750 nm, beyond that achievable with compressively strained GaInP quantum well (QW) lasers. Early developments on InP–GaInP QDs grown by solid-source molecular beam epitaxy, reported threshold current densities of $2.3 \, \text{kA} \, \text{cm}^{-2}$ for 2 mm long devices emitting at 728 nm [1]. Devices grown by metal–organic vapour phase epitaxy (MOVPE), operating at a shorter wavelength of 645 nm, were reported for 200 μm long cavities with threshold currents of $4.25 \, \text{kA} \, \text{cm}^{-2}$ [2]. These current densities were much higher than those achieved with InAs QDs which, around that time, were as low as $26 \, \text{A} \, \text{cm}^{-2}$ [3]. It was later realized that the shortcoming of InP QD lasers was related to the design and growth parameters, and particularly the growth temperature [4]. Previous MOVPE growth runs were carried out to maximize the dot density at temperatures between 580 and 650 °C, however increasing this to the region of 700 °C reduced the dot density but vastly improved the material quality and as a result 2 mm long lasers emitting at 741 nm were fabricated with record low threshold
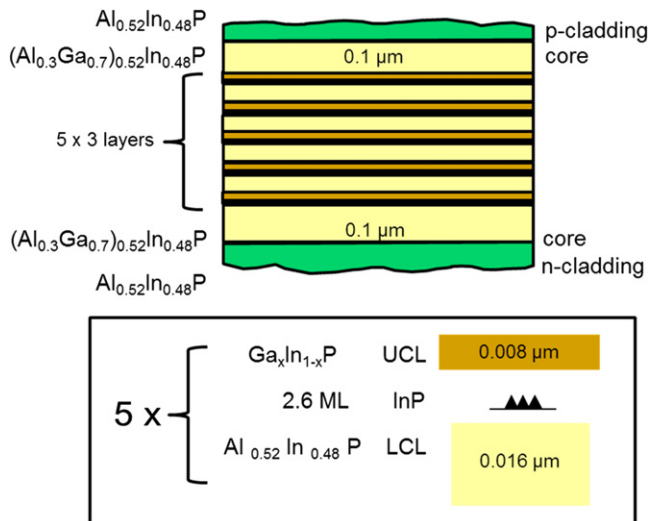
Figure 1. Schema of epitaxial structure. Active region contains five layers of dots, where each layer is deposited on a lower confining layer (LCL) or barrier layer of $(Al_{0.3}Ga_{0.7})_{0.52}In_{0.48}P$, with the upper confining layer (UCL) being composed of $Ga_xIn_{1-x}P$. The core structure is then clad with 1000 nm wide $Al_{0.52}In_{0.48}P$.

currents of 190 A cm^{-2} at 300 K [5, 6]. Reducing the growth rate of the dots has been shown to promote the formation of larger dots and this has extended the range over which optical gain can be achieved to slightly beyond 780 nm. However, to date this has been at the expense of a larger number of defects and low levels of gain at relatively high current densities [6].

Further optimization studies have revealed how the width of the barrier layer separating each dot layer can affect device performance and how the incorporation of strain in the upper confining layers of the dots can reduce the threshold current temperature dependence [7, 8]. With improvements in performance, these sources are becoming attractive for biomedical uses, since this wavelength regime minimizes the scattering, absorption and auto-fluorescence of bio-substrates. Such applications include activation of photosensitizers used in photodynamic therapy for the treatment of certain cancers, and excitation of fluorescent dyes used in imaging and diagnostics via bio-conjugation.

Growth by self assembly inherently gives rise to a fluctuation in dot size and, as such, the energy states of the ensemble are inhomogeneously broadened. Although not desirable in all respects, it means that optical gain can be achieved over a relatively large spectral range, and this enables an array of device applications. For example, a broad gain spectrum can be used to generate ultra-short light pulses from mode-locked lasers [9] or source multiple wavelengths, by using the appropriate feedback mechanisms. Here, we describe what determines the accessible range of lasing wavelengths that can be achieved using InP QDs, by either varying the active core structure or the design of the fabricated laser device.

The nature of QDs (namely the broad gain-spectra and the fast carrier dynamics [10]), lends itself as a suitable active material for dual-wavelength lasers and these traits have already been exploited in an InAs based material system

[11, 12]. In these devices dual-mode operation typically comes from the ground and first excited state transitions. InP QD laser structures exhibit a gain spectrum which is not only broad but also relatively flat-topped, due to the wide distribution of energy states. We exploit these properties to demonstrate dual-wavelength lasers which have been designed to access a range of difference-wavelengths from a single epitaxial structure. These devices are useful in a number of applications, including read/write devices for optical storage, interferometric measurements, THz emitters by difference frequency generation and bio-photonic applications [13].

2. Epitaxial structure

The InP QD laser structures were grown at the National Centre for III-V Technologies in Sheffield by low pressure MOVPE in a horizontal flow reactor. The recipe used for the growth conditions was based on those previously used to produce InP QD lasers with low threshold currents [4]. The constituents of the epitaxial structure (illustrated schematically in figure 1) were deposited on *n*-GaAs (100) substrates oriented 10° off toward $\langle 111 \rangle$. Self-assembled dots were formed by depositing 7.8 Å of InP, at a rate of 2.5 monolayers per-second, on $(Al_{0.3}Ga_{0.7})_{0.52}In_{0.48}P$ and then covered with 8 nm $Ga_xIn_{1-x}P$ QWs (upper confining layers of the dots). Structures contained five layers of dots in wells (D-WELL)s where each D-WELL layer was separated by 16 nm wide $(Al_{0.3}Ga_{0.7})_{0.52}In_{0.48}P$ barrier layers. Forming the rest of the waveguide are 1000 nm wide $Al_{0.52}In_{0.48}P$ cladding layers.

It is well known that under certain growth conditions there is a tendency for the formation of alternating monolayers (CuPt ordering) of group III atoms in both AlGaInP and GaInP [14–16] and similar effects have also been observed within other material systems such as AlGaAs [17]. This has been controlled by the use of substrates orientated away from (100) by our group [18] and others [19, 20] and fully disordered material is obtained here using a combination of off-axis substrates and growth temperature. The use of off-axis substrates under certain growth conditions can give rise to step-bunching and nano-faceting, leading to the growth of wire-like structures or dots elongated along one axis [21]. To confirm this was not the case using our growth conditions and that the emission from the dots was fully isotropic, we measured the unamplified spontaneous emission emitted out of the growth plane [e.g. 23] as a function of angle. The amplitude and spectrum of surface emitted light with transverse electric, TEx and TEy, polarizations and light polarized at 45° to these polarizations were identical, once the different collection efficiencies in the experiment were taken into account. This was achieved by normalizing to the light emitted at energies corresponding to the QWs, which we expect to be isotropic.

Atomic force microscopy (AFM) measurements of a similar structure in this series of growths revealed a bi-modal distribution of dot sizes [22] and transmission electron microscopy (TEM) has been used to determine the presence
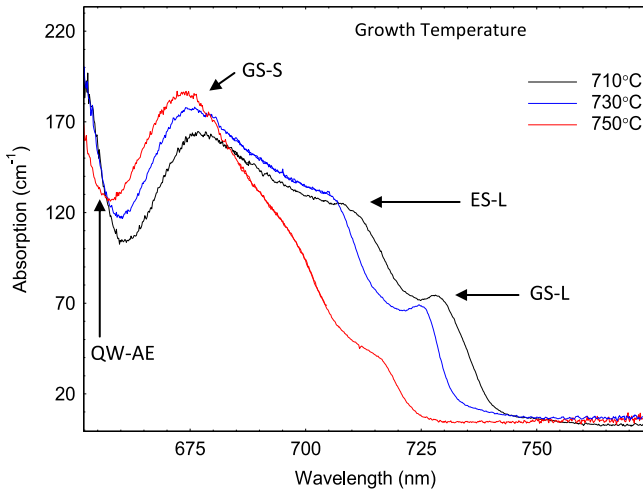
Figure 2. Optical loss spectra (sum of modal absorption plus internal optical loss) for InP/AlGaInP QD structures grown at temperatures of 710, 730 and 750 °C. GS-L and ES-L indicate the ground and exited states of the large dot subset respectively and GS-S indicates the ground state of the small dot subset.

Figure 3. Lasing wavelengths (blue circles) of 3 mm long lasers with cleaved uncoated facets, and transition energies (red squares) taken from the GS absorption peak of the large inhomogeneously QDs for various concentrations of Ga in the upper confining layer. Inset shows the corresponding threshold current density (J_{th}) versus temperature for the lasers.

of dot-like structures in a series of growths [8]. Although AFM images are useful for identifying the dots and the form of the size distribution, the exact dimensions may not be representative of those dots formed in a complete growth (as with TEM). The samples selected for imaging are uncapped and the effect of post-growth cooling is believed to promote accumulation of surface species modifying the dot dimensions [4]. A comprehensive structural characterization of a material system comprising InP embedded in $(Al_xGa_{1-x})_{0.51}In_{0.49}P$, carried out by Schulz *et al* revealed the presence of dot structures which in a majority of cases formed a bi-modal size distribution [19].

3. Experiment and results

Characterizing the optical properties of each structure allows us to determine the accessible range of wavelengths and is a prerequisite to designing a dual-wavelength laser. To this end, samples were fabricated into 50 μm wide oxide-isolated stripe segmented contact test structures. All devices have uncoated as-cleaved facets and were operated pulsed, with a pulse length of 1000 ns and a duty cycle of 0.1% to avoid self-heating. Measurements using the segmented contact method, which is an electrical version of the well-known single pass optical stripe length method, allow us to determine the internal optical mode loss, α_i, the net modal gain spectra and the unamplified spontaneous emission rate spectra [23].

Modal absorption spectra are plotted in figure 2 for InP/AlGaInP QD samples grown at three different temperatures. The presence of the GaInP QW is evident by its absorption edge (AE) labelled in the left of the figure, with the remaining features resulting from energy states formed by a bimodal distribution of dot sizes. The two features at the lower energies, labelled GS-L and ES-L, correspond to the inhomogeneously broadened ground and excited states of the large
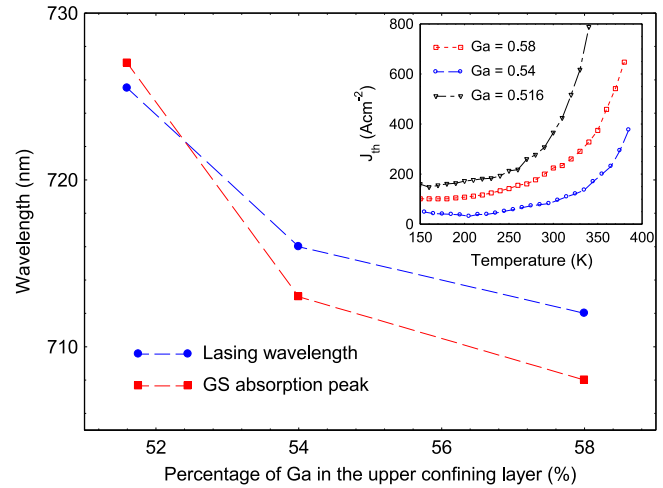
dot subset [24]. The feature labelled GS-S represents, what is believed to be, the ground state of the small dot subset. As explained in [7], the dots states are observed to blue-shift with increasing growth temperature, correlating with the effect temperature has on the size of the dots formed. The QW AE, on the other hand, remains relatively unaffected by the growth temperature. The magnitude of the modal absorption at the ground state reduces with increasing growth temperature and since the modal absorption reflects the gain which would be achieved if all the states were inverted, we can see that increasing the growth temperature reduces the maximum available gain from the GS emission of the large dots, i.e. the density of large dots has decreased. This means that the penalty to pay for reducing the operating wavelength by increasing the temperature is a material with a lower maximum gain.

A second approach to tuning the lasing wavelength is to incorporate strain in the upper-confining layers of the dots, which has the effect of shifting the optical transition energies. In these structures, the upper confining layer, comprising $Ga_xIn_{1-x}P$, creates a 2D (QW) confinement for the charge carriers and therefore acts as a reservoir supplying the dot states. As described in [8], the degree of strain is controlled by altering the fraction (x) of Gallium (Ga). For a Ga fraction of 0.516 the upper confining layer is lattice matched to GaAs. Above this value, the layer is under tensile strain (with respect to GaAs) and below it is compressive, causing the transition energy of the dots to increase or decrease respectively. There is however a compromise to be made by extending the range of emission wavelengths in this way, in that a high level of strain can have deleterious effects on material quality, increasing the threshold current of the lasers. Incorporating compressive strain into the upper confining layer of the dots (which are already compressively strained) causes material defects substantial enough that lasing at room temperature
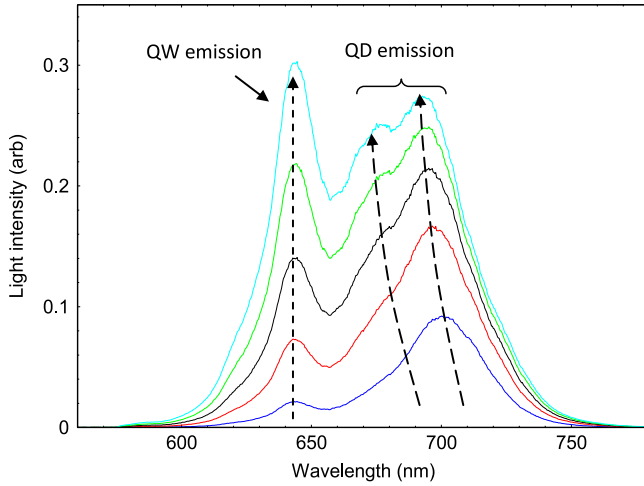
Figure 4. Unamplified spontaneous emission spectra of InP/AlGaInP QDs measured for a range of injection current (direction of increase indicated by dashed arrows).

Figure 5. Measured net modal gain spectra (G-α_i), for increasing current density (direction indicated by dashed arrow) at 300 K, showing blue-shift of gain-peak wavelength ($\Delta\lambda_{pk}$).

Figure 6. Schema of dual-wavelength laser, based on a two-section ridge waveguide. Diagram shows how the design of the device forms two effective cavities.

was not observed for a Ga fraction of 0.43. The plot in figure 3 shows how the peak of the GS absorption wavelength and how the lasing wavelength measured on 3 mm long devices with uncoated facets shifts with the concentration of Ga in the upper-confining layer. The inset shows the corresponding temperature dependence of the threshold current density for 3 mm long lasers with uncoated facets. Increasing the fraction of Ga results in a shift of the dots states to shorter wavelength and causes a similar shift in the lasing wavelength. As the Ga composition increases from 52 to 54%, there is a reduction in the threshold current density, measuring 89 A cm^{-2} at 300 K and 186 A cm^{-2} at 350 K. The threshold current density then increases with 58% Ga, as the magnitude of the modal absorption at the ground state reduces and becomes less well defined, due to the number of dot state transitions reducing and being more inhomogenously broadened at the highest Ga compositions. As 54% Ga produced the best performance in terms of threshold current characteristics, this sample was selected to fabricate a dual-wavelength laser and all further measurements described in this paper were made on this structure.

Unamplified spontaneous emission spectra can be used to identify the range of wavelengths over which states are populated. Data for spontaneous emission, obtained through a 50 μm by 4 μm top window etched through the metallization and p-doped cap on the top of the sample [25], is shown in figure 4 for a temperature of 300 K. The region of the spectrum which corresponds to emission from the dot states (660 to 750 nm), previously identified using modal absorption and edge-photovoltage spectra [8], clearly shows the effect of state-filling and a shifting of the peak positions with increasing injection. At high injection, emission from the dots begins to saturate and recombination from the QW states around 650 nm begins to dominate, with the peak wavelength remaining almost fixed due to the relatively large number of QW states.

The lasing wavelength is controlled by the amount of gain available to compensate the threshold losses of the laser
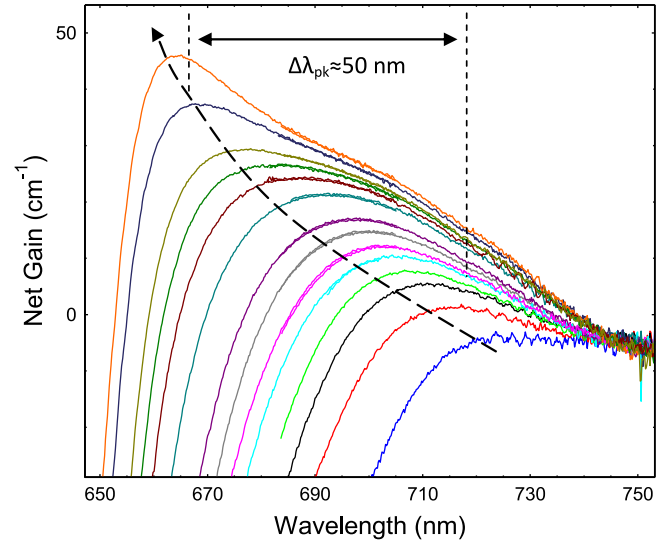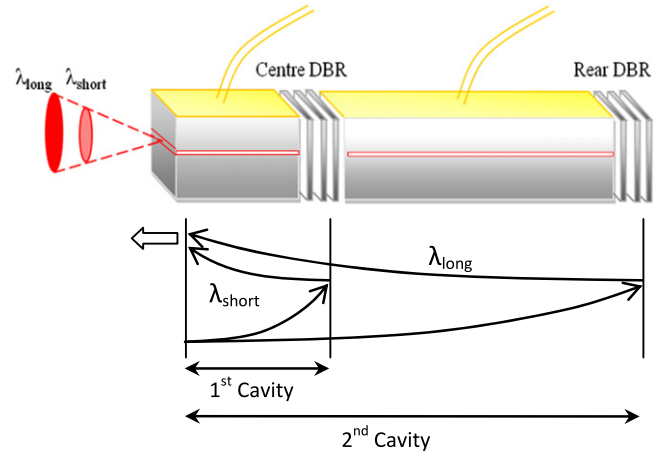
cavity. The modal gain spectrum, shown in figure 5, was measured for a range of injection currents at 300 K. The gain-peak wavelength is observed to blue-shift with increasing carrier injection as the inhomogeneously broadened dot states become populated. From this it is apparent that the gain requirement, determined from the loss imposed by the cavity, can have a significant effect on the operating wavelength of the laser. Measurements of modal gain spectra allow us to establish the extent of the blue-shift which can be achieved by varying the mirror loss, and hence determine the upper limit of the difference-wavelength in a dual-wavelength laser.

To demonstrate how simultaneous dual-wavelength lasing can be achieved by accessing various dot states, we fabricated devices (example schema shown in figure 6) based on a ridge-waveguide geometry which consists of two sections. These sections are separated by a deep-etched distributed Bragg reflector (DBR) which is designed to be reflective at
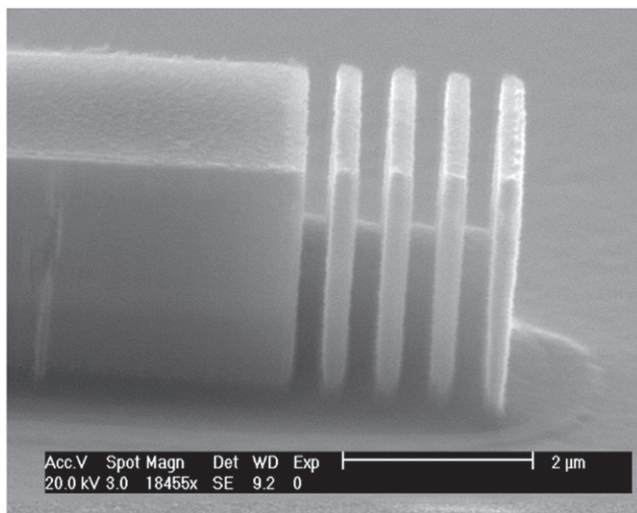
Figure 7. SEM micrograph of a ridge-waveguide and DBR etched into InP/AlGaInP.

Figure 8. Measured emission spectra for dual-wavelength lasers with various difference-wavelengths.

short wavelengths and transmitting at longer wavelengths. This effectively creates two cavities of different loss values, with the short wavelength light oscillating over the first section and the longer wavelength oscillating over the entire length of the device. To allow the two sections to be pumped independently, they are isolated electrically by ensuring that the etched portions of the grating extend down to the substrate, approximately $3 \mu m$, with a period typically of 450–500 nm depending on the stop-band required. In addition, by etching to this depth, the contrast in refractive index between each of the grating portions is vertically symmetric on the scale of the optical mode, preventing light from being guided towards the substrate, as with surface-etched gratings. Typically, the ridge-waveguides are $4 \mu m$ wide and the section lengths are between 300 and $800 \mu m$ for the short section and 1000–$2000 \mu m$ for the long section. The actual length chosen depends on the losses required, and hence which dot states are utilized for lasing.

Light from both wavelengths is collected from the front of the first section, which is defined by a cleaved facet. The second section of the device has a DBR placed at its end to increase reflectivity at the longer wavelength. An SEM micrograph of a typical DBR is shown in figure 7. The grating is etched down to the GaAs substrate using an Oxford Instrument Plasmalab 100 system with an ICP380 chamber design. The third order gratings can be made reproducibly once the conditions necessary to achieve directional etching with good aspect ratio are determined.

Here etching was performed using a simple gas chemistry of Ar/Cl_2 in a ratio of 9:1 with the sample being held at a temperature of $200\,°C$ to enhance the removal of the etch product, $InCl_3$. The etched portions of the grating were filled in with benzocyclobutene during the planarization process.

The loss of the two cavities can be altered by changing the length of the sections and the reflectivity spectrum of the centre DBR. The two lasing wavelengths are determined by the wavelength at which the gain matches the losses imposed
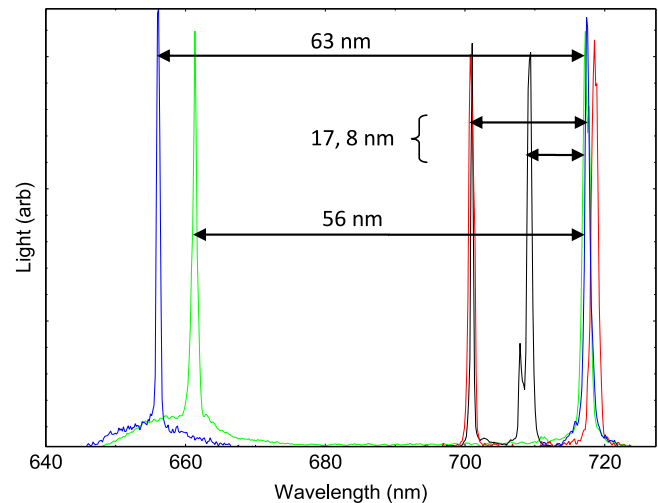
by each cavity. The mirror loss (or net gain requirement) of each cavity can be calculated from the round-trip gain equation. The design of the DBR reflectivity spectrum, computed from a *transfer matrix model*, is chosen such that when inserted into the equation it produces the desired spectrally dependent mirror-loss. Moreover, since the form of the gain spectrum (with increasing carrier injection) has been fully characterized, the wavelength at which the gain overcomes the loss can be determined. Due to the large blue-shift of the gain peak wavelength with carrier injection, the design of the DBR and cavity lengths can be engineered to produce various pairs of lasing wavelength. The plot in figure 8 shows an example of pairs of lasing wavelengths, with a maximum separation of 63 nm.

As discussed earlier, within this wavelength regime, the dual-wavelength laser is attractive for biomedical sensing. The advantage of this design is the large range of difference wavelengths that can be achieved and this makes it suitable for excitation of fluorescent dyes or fluorochromes, as used in devices such as flow cytometers. There are numerous distributed feedback (DFB) based dual-wavelength lasers which can be used for generating multiple wavelengths, but the optical modes are often spatially separated, such as in chirped DFB arrays or laterally coupled DFBs [26, 28]. In cases where the two wavelengths are generated along the same optical axis, the sections of the device need to be electrically isolated for asymmetric pumping of the gain medium. With deep-etched grating, as used here, this is achieved as a result of etching through the metallurgical junction. Another approach which can be used for electrical isolation, but at the expense of increasing fabrication complexity, is ion bombardment [11]. Laser diodes used in flow cytometers such as *Navios* and *Gallios* produced by *Beckman Coulter* can operate effectively at optical powers as low as 20 mW, a power output which is readily achievable with this device. The spectral width of each lasing mode is not as narrow as that which could be achieved with DFB lasers, but for biomedical applications which make use of *fluorochromes*, the
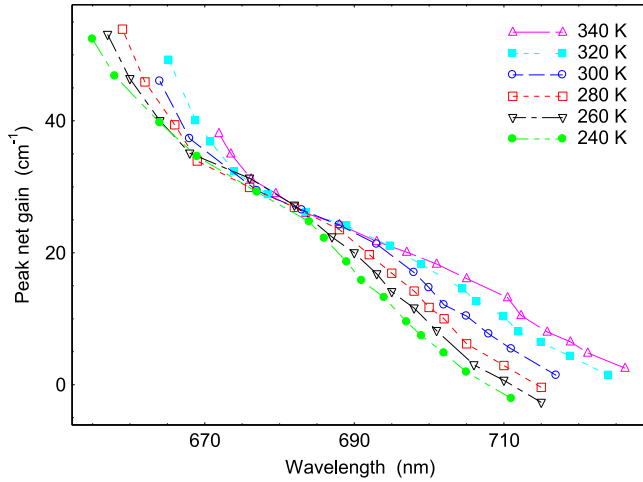
Figure 9. Plot shows relationship between the peak net-gain and its spectral position. For gain values in the region of 25–30 cm^{-1} there is little change in the gain peak wavelength with temperature.

Figure 10. Lasing wavelength versus temperature for dual-wavelength lasers with 63 nm (blue circles) and 8 nm (red squares) difference-wavelength at 300 K.

targeted absorption peaks are relatively broad so spectral purity is not a limiting factor.

In some applications it is useful to be able to tune the difference-wavelength. While the lasing wavelengths are set by the optical loss determined by the structural parameters set during the fabrication, there is still a mechanism to fine tune the difference-wavelength using the operating temperature. In QD material the temperature sensitivity of the operating wavelength is dependent on the absolute magnitude of the optical loss of the laser, as explained in [27]. The effect is illustrated in figure 9, where the magnitude of the net modal-gain is plotted as a function of wavelength of the peak of the gain spectrum from 240 to 340 K. It is worth noting that when a certain value of gain (approximately 25 cm^{-1}) is reached, the gain-peak wavelength becomes relatively insensitive to temperature and this has been used to produce lasers with temperature dependences as low as 0.03 nm K^{-1} (measured from 240 to 380 K) [27].

In dual wavelength lasers the magnitude of the cavity losses are different to produce the different wavelengths and this naturally also provides a difference in wavelength change with temperature. The temperature dependence of the lasing wavelengths for devices with 300 K wavelength separations of 63 and 8 nm are plotted in figure 10, and have a temperature tuning of 0.11 nm K^{-1} and 0.12 nm K^{-1} respectively. These values are a result of both the effect seen in figure 9 (due to the property of the QDs) and the temperature dependence of the DBR stop-band.

Standard diode lasers do not typically produce lasing action at just two wavelengths but when they do, the intensity at each wavelength tends to be very sensitive to the operating current and temperature, leading to the intensity at one of the two wavelengths dominating. Several approaches have been suggested to improve the stability of dual wavelength operation, usually by avoiding lasing in the same spatial position, as a means to avoid or reduce the effect of direct competition of the two lasing processes for the same inverted carrier population [e.g. 28–31]. However, in applications
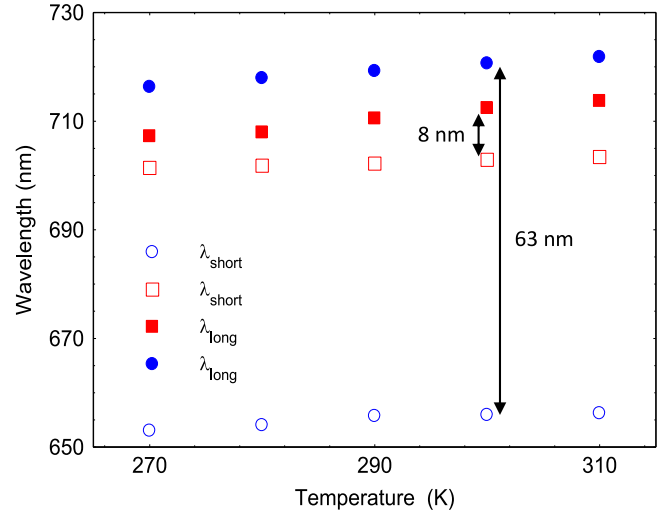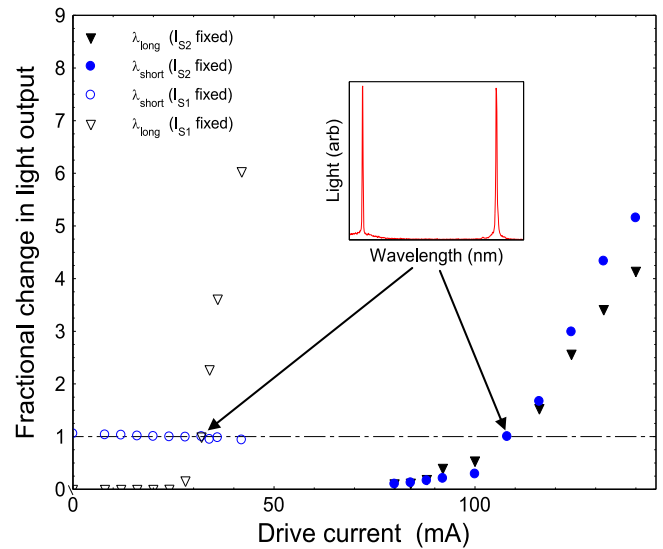

Figure 11. Fractional change in light intensity at each wavelength (λ_1, λ_2) when varying current (*I*) in one section while held constant in the other. Arrows indicate point where the light intensity in each mode was equal. Difference wavelength measured to be 63 nm.

which require two wavelengths, lasing at different spatial locations can add practical complexities.

For purely independent lasing to be realized, the modes must not interact with the same excited carrier population. Previous work has illustrated that this can be achieved with QD material, providing the two energies are separated by more than the homogenous linewidth [32]. Alternatively, this can be viewed as a requirement that carriers must recombine on a timescale which is less than the time taken for carriers to redistribute between the two carrier populations.

To investigate the stability of the intensity at the two wavelengths, the light level at each wavelength was initially set to be equal by adjusting the current to each section. Then, as the current in one of the two sections was varied, while the other was held constant, the fractional change in light output

at each wavelength was measured. The data in figure 11 was obtained for a difference-wavelength of 63 nm. In this device the light level at the short wavelength remains relatively constant for changes in current applied to section two. This is because the long wavelength operates at a low level injection, so the number of carriers that the mode is competing for (over the length of section one) is small compared to the number required to sustain lasing at the short wavelength.

Carriers injected into section one can be stimulated to recombine at either wavelength and so varying the current to this section affects the light output of both lasing modes. In addition, light outside the centre DBR stop-band may be transmitted into section two causing optical pumping of that section (at a high photon energy), thereby increasing the lasing output at the long wavelength.

4. Conclusions

In summary, we have briefly discussed the mechanisms by which growth temperature and the incorporation of strain in the upper confining layer affects the peak transition energy of InP QDs and threshold currents of edge-emitting lasers. We explored the range of operating wavelengths which could be accessed in this material system and used optical gain measurements to establish how the gain-peak wavelength varies with carrier injection, via the effects of state-filling. Using the optical loss as a mechanism to vary the emission wavelength has allowed the demonstration of dual-wavelength lasers with various mode separations from 8 to 63 nm. Tuning of the difference-wavelength could be achieved by simply varying the operating temperature of the device. Finally, the stability of each emitting wavelength to variations in drive current was investigated. Results show that the short wavelength is relatively insensitive to changes in the light output at the long wavelength for large wavelength separations.

Acknowledgments

References

[1] Manz Y M, Schmidt O G and Eberl K 2000 Room temperature lasing via ground state of current injected vertically aligned InP/GaInP quantum dots *Appl. Phys. Lett.* **76** 3343–5

[2] Walter G, Elkow J, Holonyak N, Heller R D, Zhang X B and Dupuis R D 2004 Visible spectrum (645 nm) transverse electric field laser operation of InP quantum dots coupled to tensile strained $In_{0.46}Ga_{0.54}P$ quantum wells *Appl. Phys. Lett.* **84** 666–8

[3] Liu G T, Stintz A, Li H, Malloy K J and Lester L F 1999 Extremely low room-temperature threshold current density diode lasers using InAs dots in $In_{0.15}Ga_{0.85}As$ quantum well *Electron. Lett.* **35** 1163–5

[4] Krysa A B, Liew S L, Lin J C, Roberts J S, Lutti J, Lewis G M and Smowton P M 2007 Low threshold InP/AlGaInP on GaAs QD laser emitting at ≈740 nm *J. Cryst. Growth* **298** 663–6

[5] Lutti J, Smowton P M, Lewis G M, Krysa A B, Roberts J S, Houston P A, Xin Y C, Li Y and Lester L F 2005 740 nm InP–GaInP quantum-dot laser with 190 A cm^{-2} room temperature threshold current density *Electron. Lett.* **41** 247–8

[6] Smowton P M, Lutti J, Lewis G M, Krysa A B, Roberts J S and Houston P A 2005 InP–GaInP quantum-dot lasers emitting between 690 and 750 nm *IEEE J. Sel. Top. Quantum Electron.* **11** 1035–40

[7] Smowton P M, Al-Ghamdi M S, Shutts S, Edwards G, Hutchings M and Krysa A B 2010 Effect of growth temperature on InP QD lasers *IEEE Photonics Technol. Lett.* **22** 88–90

[8] Elliott S N, Smowton P M, Krysa A B and Beanland R 2012 The effect of strained confinement layers in InP self-assembled quantum dot material *Semicond. Sci. Technol.* **27** 094008

[9] Kuntz M, Fiol G, Laemmlin M, Meuer C and Bimberg D 2007 High-speed mode-locked quantum-dot lasers and optical amplifiers *Proc. IEEE* **95** 1767–78

[10] Langbein W, Cesari V, Masia F, Krysa A B, Borri P and Smowton P M 2010 Ultrafast gain dynamics in InP quantum-dot optical amplifiers *Appl. Phys. Lett.* **97** 211103

[11] Naderi N A, Grillot F, Yang K, Wright J B, Gin A and Lester L F 2010 Two color multi-section quantum dot distributed feedback laser *Opt. Express* **18** 27028–35

[12] Daghestani N S, Cataluna M A, Ross G and Rose M J 2011 Compact dual-wavelength InAs/GaAs quantum dot external-cavity laser stabilized by a single volume Bragg grating *IEEE Photonics Technol. Lett.* **23** 176–8

[13] Qin J, Reif R, Zhi Z, Dziennis S and Wang R 2012 Hemodynamic and morphological vasculature response to a burn monitored using a combined dual-wavelength laser speckle and optical microangiography imaging system *Biomed. Opt. Express* **3** 455–66

[14] Gomyo A, Suzuki T, Kobayashi K, Kawata S, Hino I and Yuasa T 1987 Evidence for the existence of an ordered state in $Ga_{0.5}In_{0.5}P$ grown by metalorganic vapour phase epitaxy and its relation to band-gap energy *Appl. Phys. Lett.* **50** 673–5

[15] Bellon P, Chevalier J P, Augarde E, Andre J P and Martin G P 1989 Substrate-driven ordering microstructure in $Ga_xIn_{1-x}P$ alloys *J. Appl. Phys.* **66** 2388–94

[16] Kondow M, Kakibayashi H, Minagawa S, Inoue Y, Nishino T and Hamakawa Y 1988 Crystalline and electronic energy structure of OMVPE-grown AlGaInP/GaAs *J. Cryst. Growth* **93** 412–7

[17] Löffler A, Reithmaier J-P, Forchel A, Sauerwald A, Peskes D, Kümmell T and Bacher G 2006 Influence of the strain on the formation of GaInAs/GaAs quantum structures *J. Cryst. Growth* **286** 6–10

[18] Lewis G M, Lutti J, Smowton P M, Blood P, Krysa A B and Liew S L 2004 Optical properties of InP/GaInP quantum-dot laser structures *Appl. Phys. Lett.* **85** 1904–6

[19] Schulz W-M, Roßbach R, Reischle M, Beirne G J, Bommer M, Jetter M and Michler P 2009 Optical and structural properties of InP quantum dots embedded in $(Al_xGa_{1-x})_{0.51}In_{0.49}P$ *Phys. Rev. B* **79** 035329

[20] Porsche J, Ruf A, Geiger M and Scholz F 1998 Size control of self-assembled InP/GaInP quantum islands *J. Cryst. Growth* **195** 591–5

[21] Shchukin V A, Ledentsov N N, Soshnikov I P, Kryzhanovskaya N V, Maximov M V, Zakharov N D, Werner P and Bimberg D 2006 Nanofaceting and alloy decomposition: from basic studies to advanced photonic devices *Microelectron. J.* **37** 1451–60

[22] Lutti J, Smowton P M, Lewis G M, Blood P, Krysa A B, Lin J C, Houston P A, Ramsay A J and Mowbray D J 2005

Gain saturation in InP/GaInP quantum-dot lasers *Appl. Phys. Lett.* **86** 011111

[23] Blood P, Lewis G M, Smowton P M, Summers H D, Thomson J D and Lutti J 2003 Characterisation of semiconductor laser gain media by the segmented contact method *IEEE J. Sel. Top. Quantum Electron.* **9** 1275–82

[24] Al-Ghamdi M S, Smowton P M and Blood P 2011 Dot density effect by quantity of deposited material in InP/AlGaInP structures *IEEE Photonics Technol. Lett.* **23** 1169–71

[25] Blood P, Fletcher E D, Hulyer P J and Smowton P M 1986 Emission wavelength of AlGaAs–GaAs multiple quantum well lasers *Appl. Phys. Lett.* **48** 1111

[26] Li W, Zhang X and Yao J 2013 Experimental demonstration of a multiwavelength distributed feedback semiconductor laser array with an equivalent chirped grating profile based on the equivalent chirp technology *Opt. Express* **21** 19966–71

[27] Shutts S, Smowton P M and Krysa A B 2013 InP quantum dot lasers with temperature insensitive operating wavelength *Appl. Phys. Lett.* **103** 061106

[28] Pozzi F, De La Rue R M and Sorel M 2006 Dual wavelength InAlGaAs–InP laterally coupled distributed feedback laser *IEEE Photonics Technol. Lett.* **18** 2563–5

[29] Price R K, Verma V B, Tobin K E, Elarde V C and Coleman J J 2007 Y-branch surface etched distributed Bragg reflector lasers at 850 nm for optical heterodyning *IEEE Photonics Technol. Lett.* **19** 1610–2

[30] Kaspi R, Onstad A P, Dente G C, Tilton M L and Tauke-Pedretti A 2008 Optically pumped mid-infrared laser with simultaneous dual wavelength emission *IEEE Photonics Technol. Lett.* **20** 1467–9

[31] Ito S, Suehiro M, Hirata T and Hidaki T 1995 Two longitudinal-mode laser diodes *IEEE Photonics Technol. Lett.* **7** 959–61

[32] Sugawara M, Mukai K, Nakata Y, Otsubo K and Ishikawa H 2000 Performance and physics of quantum dot lasers with self assembled columnar shaped and 1.3 μm emitting InGaAs quantum dots *IEEE J. Sel. Top. Quantum Electron.* **6** 462–74